Pergamon

PII: S0022-3697(97)00095-4

J. Phys. Chem Solids Vol 58, No. 11, pp. 1833–1837, 1997

0022-3697/97 $17.00 + 0.00

ELECTRONIC PROPERTIES OF CARBON NANOTUBES CONTAINING DEFECTS

PH. LAMBIN[a], A.A. LUCAS[a] and J.C. CHARLIER†[b]

[a]Département de Physique, Facultés Universitaires Notre-Dame de la Paix, B-5000, Namur, Belgium
[b]IRRMA, Ecole polytechnique de Lausanne, INR–Ecublens, CH-1015, Lausanne, Switzerland

Abstract—The electronic structure of carbon nanotubes containing defects is investigated within a tight-binding framework. The electronic properties of the following defects are examined: (a) a hemispheric cap ending a (10, 10) tubule, (b) a pair of pentagon and heptagon aligned along the same side of the tube, which widens the diameter, (c) a pair of diametrically-opposed heptagon and pentagon, which bends the structure, and (d) sp^3-like lines responsible for polygonization. In cases (a)–(c), a structural optimization was performed, either by minimization of a valence-force field adapted to the carbon network or by tight-binding molecular dynamics.

1. INTRODUCTION

The electronic structure of ideal carbon nanotubes is well understood: For a single-shell tubule with not too small diameter, the rule is that a metallic or semiconducting system is obtained whether or not $l - m$ is a multiple of three, where l and m are the two integral components of the so-called chiral vector [1–3]. In comparison, very little is known about the influence that defects have on the electronic structure of the nanotubes, and how they can be important for some potential applications. For instance, the presence of caps at both ends of a nanotube is the most obvious deviation from the ideal, rolled-up graphene sheet [4]. As far as applications are concerned, the field-emission properties of carbon nanotips depend sensitively on how their electronic structure evolves towards the apex of their caps [5].

In some samples, high-resolution transmission electron microscopy (TEM) revealed changes in the tube diameter [6]. Also, coiled structures have been observed where sharp bends take place between straight tubule portions [7]. It is believed that pairs of heptagons and pentagons incorporated in the otherwise perfect honeycomb C network lead to such defected tubules [8]. Now to come back to applications, a pentagon–heptagon pair makes it possible to connect metallic and semiconducting nanotubes, opening the way to possible devices working at the nanoscale [9, 10].

Other TEM images of some carbon nanotubes revealed the presence of non-symmetric lattice fringes, suggesting that in these instances, the tube cross sections are polygonal and not circular [11]. Rows of carbons along the polygonal edges acquire some sp^2 character that contrasts with the mostly sp^2 bonding of the rest of the atoms, and this rehybridization influences the electronic structure of the tubule, as discussed below.

It is the purpose of the present paper to illustrate on a few examples how the electronic structure of single-shell nanotubes is affected by the above-mentioned defects. Except for the nanotubes with polygonized cross sections, which were treated differently, the electronic densities of states (DOS) of the defected tubules were computed with a tight-binding Hamiltonian restricted to the carbon π orbitals, given that the π states indeed control the electronic structure of the carbon tubules near the Fermi level [3]. Only first-neighbor C–C interactions were considered, with the two-center hopping integral $V_{pp\pi}$, set at the experimental value -3.1 eV. The local DOSs were obtained by application of the recursion method [12] up to 150 levels in the continued-fraction expansion of the Green function, corresponding to 300 exact moments. A small imaginary part (0.04 eV) was added to the energy for making the continued fractions convergent.

2. ELECTRONIC STRUCTURE OF A CAPPED NANOTUBE

The variations of the π density of states along a capped nanotube is illustrated here for the case of a (10, 10) tubule terminated with half a C_{240} molecule. This system was selected for its relevance to the crystalline ropes of metallic nanotubes recently produced by laser ablation [13]. These nanotubes were shown by TEM to be perfectly closed by hemispheric caps. Since the individual nanotubes in a rope are parallel and have all the same length, the ropes could constitute good field-emission arrays [5].

†Permanent address: PCPM, Université Catholique de Louvain, 1 place Croix du Sud, B-1348, Louvain-La-Neuve, Belgium.

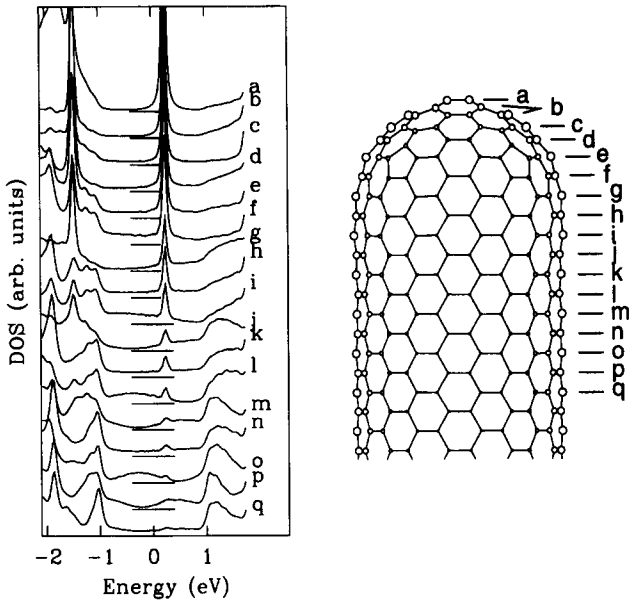

Fig. 1. Local densities of π-electron states along a (10, 10) nanotube capped with half a C_{240} molecule. The horizontal bars indicate zero densities. The Fermi level is at zero energy. The DOS curves are averaged over the atoms composing the sections labeled by *a*...*q* in the structure drawn on the right-hand side, which has been projected on a plane containing the fivefold axis.

Based on these observations, a structural model was built on the computer where half a C_{240} with a pentagon at the top was attached to a (10, 10) nanotube and relaxed by tight-binding molecular dynamics [14]. Fig. 1 illustrates the atomic structure obtained. The curves on the left-hand side are the local densities of π electron states averaged over the sections labeled a (pentagonal apex) to *q*. A prominent peak appears just above the Fermi level E_F (located at zero energy), which is associated with the presence of the pentagon at the tip apex. In principle the tubule is already metallic but there is this huge increase of density of states near E_F toward the apex. This would imply a corresponding enhancement of the field emission current, and a feature should develop in the energy distribution of field emitted electrons from an array of such carbon nanotips.

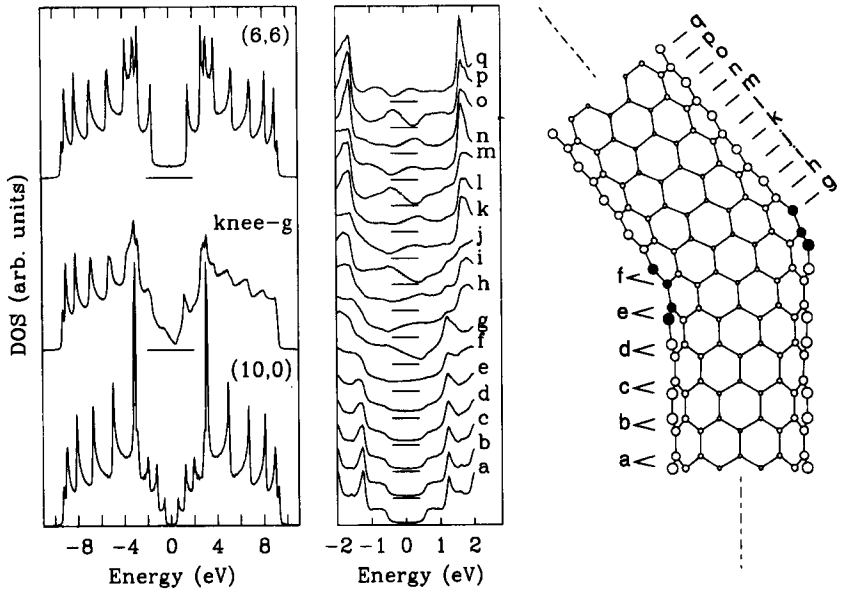

Fig. 2. Densities of π states and optimized atomic structure of the (10, 0)–(6, 6) knee, with the pentagon and heptagon represented by shaded circles. The curves labeled *a*–*q* represent the densities of states averaged over 12 or 20 atoms at the sections indicated by the corresponding letters in the right-hand side projection of the structure. The Fermi level is at zero energy. The horizontal bars indicate the zero-density levels. In the left-hand side panel, the local density of states at the section g of the knee is compared with the densities of states of the two isolated nanotubes.

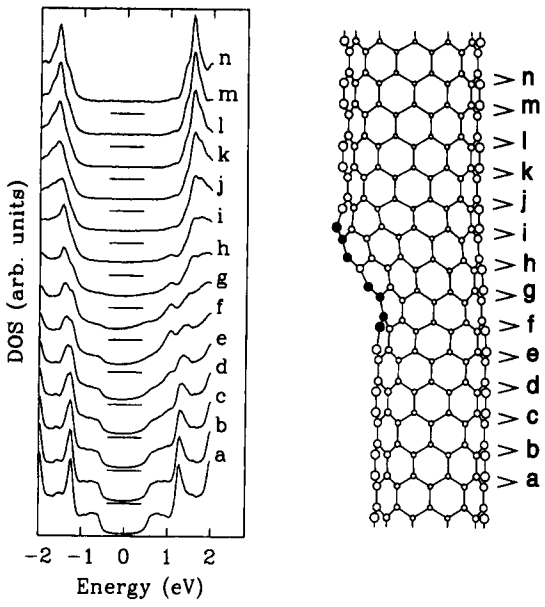

Fig. 3. Local densities of π states and optimized atomic structure of the (12, 0)–(10, 0) straight connection, projected on its symmetry plane containing the axis. The pentagon and heptagon are represented by shaded circles. The curves labeled a–n represent the DOS averaged over the zigzag sections indicated by the corresponding letters along the structure.

3. ELECTRONIC STRUCTURE OF NANOTUBE HETEROJUNCTIONS

As mentioned in the Introduction, a pentagon–heptagon pair defect makes it possible to connect nanotubes with different chiral vectors [8] (The fact that a pentagon–heptagon dipole introduces a change of chirality on cylindric hexagonal networks was already pointed out by Major et al. [15]) and, therefore, different electronic structures. Quasi one-dimensional heterojunctions could then be realized in this way, including metal-semiconductor hybrids for which interesting properties may be expected [9, 10]. When the pentagon and heptagon are positioned at two diametrically-opposed sides of the structure, the axis of the two connected nanotubes make an angle about 30° [8]. In fact bending angles of that order of magnitude have been observed experimentally in coiled nanotubes [16, 17]. The angle can be made smaller by putting the pentagon and heptagon closer to each other [18] and it is even possible to connect two different nanotubes without bending the structure by aligning the pentagon and heptagon along the same side [6, 19, 20].

The electronic structures of nanotubes hybrids have already been investigated by various techniques for different pentagon–heptagon constructions [18–21]. We comment here on the results we obtained by the recursion method for two metal-semiconductor heterojunctions. Fig. 2 shows a bent structure realized by connecting two (6, 6) and (10, 0) half nanotubes, which demands positioning the pentagon and heptagon at opposite sites of the structure. This pentagon–heptagon connection induces a rotation of the chiral vector, going here from the zigzag to armchair conformation. The structure of Fig. 2 was optimized by molecular mechanics [22], which led to a bend angle of 37° [21]. The (10, 0) zigzag nanotube is a semiconductor with a band gap of 1.1 eV, whereas the (6, 6) armchair nanotube presents a plateau of metallic π states which extends 1.6 eV on both sides of the Fermi level. The central curve in the left-hand panel of Fig. 2 shows the density of states averaged over 12 sites at the interface between the two half nanotubes (at the section labeled g). The electron–hole symmetry is lost there due to the presence of the odd-membered rings.

The central panel of Fig. 2 illustrates how the density of states around E_F varies along the (6, 6)–(10, 0) heterojunction. When going downwards away from the interface (curves e–a), the local DOS vanish progressively. At section a, the (10, 0) nanotubes has mostly recovered all of its intrinsic semiconducting properties. When moving upwards from the interface (curves h–q), the density of states oscillates around the value of the plateau. These oscillations reflect the existence of standing waves generated by those metallic Bloch states that fall within the band gap of the semiconducting system, which cannot propagate deep in the (10, 0) nanotube and are therefore reflected backwards [21]. The period of the stationary Bloch waves so generated is close to the Fermi wave vector, which for an armchair nanotube is three times the one-dimensional lattice parameter [2], hence the triple period. Notice that oscillations of that sort also develop along the capped (10, 10) nanotube, for the very same reason (Fig. 1).

Fig. 3 shows the structure of a straight connection between (12, 0) and (10, 0) zigzag nanotubes. The pentagon and heptagon are now aligned along the same side and, by contrast with the previous example, there is no change in chirality, but there is a widening of the tube diameter. The structure of Fig. 3 was optimized by tight-binding molecular dynamics [21]. The pentagon is flat and makes a small protuberance, the heptagon in the trough is boat shaped. The electronic densities of states on the successive zigzag rings of the structure indicate a continuous evolution from the metallic plateau of the (12, 0) nanotube (top) and the band gap of the (10, 0) semiconducting system (bottom). Here, like in the previous example, a continuous distribution of metal-induced gap states exist in the semiconducting system only very close to the interface with the metallic nanotube (curves c–e in Fig. 2, curves d–f in Fig. 3) [18]. Since curves a and n are already close to the DOSs of the isolated nanotubes, one concludes that the metal–semiconductor transition operates within a few C–C distances. Let us also mention that I–V curves have been determined theoretically for such heterojunctions, which show no conductance of the system within the

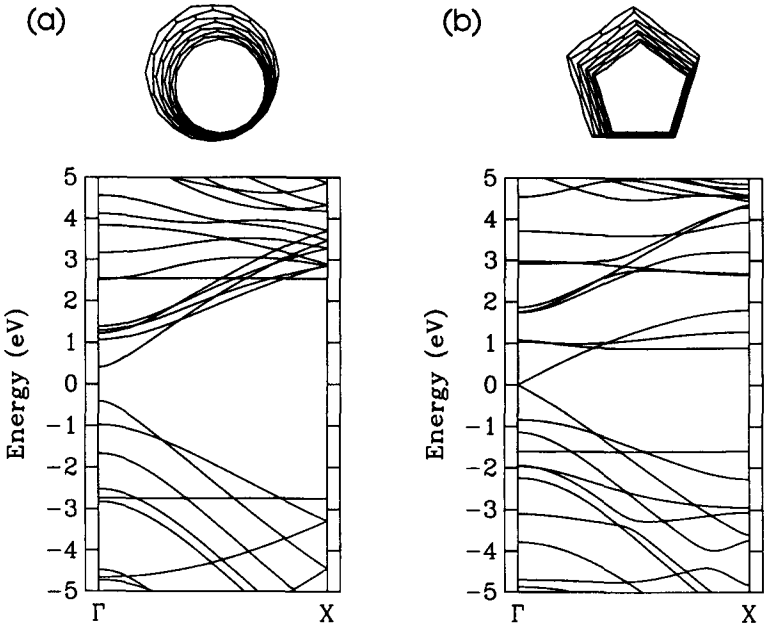

Fig. 4. Electronic band structure of a (10, 0) zigzag nanotube with a circular (a) and pentagonal (b) cross section. Both σ, and π states are represented. The zero of energy has been shifted to mid gap. The shapes of the cross sections are sketched on the top.

semiconductor gap region [19]. Since the conductivity can now be measured locally on individual nanotubes [23, 24]. It is hoped that experimental measurements will be performed for pure-C hybrids of the kind discussed here, or for heterojunctions between C and $B_xC_yN_z$, nanotubes that might reveal more appropriate for practical applications [25].

4. CARBON NANOTUBE WITH A POLYGONIZED CROSS SECTION

As briefly mentioned in the Introduction, there exist a few experimental examples that some carbon nanotubes might have a polygonal cross section [11]. Although the circular cross section is undoubtedly more stable, polygonization may be induced by pentagons in the cap [28]. It can also be the result of flattening the tubules against each other in microbundles as the consequence of the van der Waals interaction [29]. The polygonized edges can be considered as defected lines of rehybridization in the otherwise sp^2 network, with strong sp^3 character in the folds [26]. Such local variations of the carbon bonding can affect significantly the electronic structure of the nanotube [27] as illustrated below for a (10, 0) zigzag nanotube with pentagonal cross section. The edges of the pentagonal prism are taken along rows of C–C bonds parallel to the axis (see Fig. 4).

The tight-binding Hamiltonian used for this particular problem now incorporates the 2s and 2p C orbitals and includes first- and second-neighbor interactions [30]. Fig. 4 depicts the results obtained for the band structures. The (10, 0) nanotube with circular cross section is a semiconductor, with band gap 0.82 eV as given by the present Hamiltonian [31]. Polygonizing the cross section lowers the symmetry from a ten- to five-fold axis, and this lifts the degeneracy of a few bands. More importantly, the strong curvature realized near the edges of the nanoprism is responsible for a σ^*–π^* hybridization which affects drastically the electronic band structure, as already proved for the case of small-radius nanotubes [32]. Furthermore, bending hexagonal rings out of plane along the prim edges (refer to Fig. 4b) brings new pairs of atoms closer than the graphitic second-neighbor distance. This leads to additional hopping interactions in the Hamiltonian which further contribute to modify the band structure. As a consequence of all these effects, the semiconducting gap of the (10, 0) nanotube is almost completely closed when a pentagonal cross section is considered (see Fig. 4b). These tight-binding results are confirmed by ab initio calculations which predict a slightly larger gap (0.08 eV) for the same system, still much smaller than that of the circular cylinder [27]. An implication of this result is that hybridization effects could affect the electronic structure of a solid-state packing of faceted nanotubes.

5. SUMMARY

As illustrated in Sections 2 and 3, topological defects affects the electronic structure of a nanotube by destroying locally the electron–hole symmetry of the π–π^* states, or by bringing new structures in the densities of states. The perturbation can extend at a large distance away from the defect due to quantum interferences, as

revealed by the triple quasi-period of the DOS oscillations in terminated armchair nanotubes (Figs 1 and 2). As shown in Section 4, polygonizing the cross section of zigzag carbon nanotubes changes quantitatively the electronic band structure from that deduced by simply 'folding' the graphene sheet band structure.

Acknowledgements—Parts of this work have benefitted from useful discussions with L. Henrard, J.B. Nagy, A. Fonseca, and T.W. Ebbesen, who are greatly acknowledged. This work has been partly funded by the Interuniversity Research Project on 'Sciences of interfacial and mesoscopic structures' (PAI-IUAP N. P3–49). One of the authors (J.C.C.) is grateful to the National Fund for Scientific Research (FNRS) of Belgium for financial support.

REFERENCES

1. Mintmire, J.W., Dunlap, B.I. and White, C.T., *Phys. Rev. Lett.*, 1992, **68**, 631.
2. Hamada, N., Sawada, S.I. and Oshiyama, A., *Phys. Rev. Lett.*, 1992, **68**, 1579.
3. Saito, R., Fujita, M., Dresselhaus, G. and Dresselhaus, M.S., *Appl. Phys. Lett.*, 1992, **60**, 2204.
4. Iijima, S., Ajayan, P.M. and Ichihashi, T., *Phys. Rev. Lett.*, 1992, **69**, 3100.
5. de Heer, W.A., Chatelain, A. and Ugarte, D., *Science*, 1995, **270**, 1179.
6. Iijima, S., Ichihashi, T. and Ando, Y., *Nature*, 1992, **356**, 776.
7. Zhang, X.B., Zhang, X.F., Bernaerts, D., Van Tendeloo, G., Amelinckx, S., Van Landuyt, J., Ivanov, V., Nagy, J.B., Lambin, Ph. and Lucas, A.A., *Europhys. Lett.*, 1994, **27**, 141.
8. Dunlap, B.I., *Phys. Rev.*, 1994, **B 49**, 5643.
9. Service, R.F., *Science*, 1996, **271**, 1232.
10. Dresselhaus, M., *Phys. World*, 1996, **9 (May)**, 18.
11. Liu, M. and Cowley, J.M., *Carbon*, 1994, **32**, 393.
12. Haydock, B., Heine, V. and Kelly, M.J., *J. Phys. C: Solid St. Phys.*, 1975, **8**, 2591.
13. Thess, A., Lee, R., Nikolaev, P., Dai, H., Petit, P., Robert, J., Xu, C., Lee, Y.H., Kim, S.G., Colbert, D.T., Scuseria, G., Tomdnek, D., Fisher, J.E. and Smalley, R.E., *Science*, 1996, **273**, 483.
14. Goedecker, S. and Colombo, L., *Phys. Rev. Lett.*, 1994, **73**, 122.
15. Major, A., Taylor, N., Lawrence, A., Rivier, N. and Sadoc, J.F., *Phil. Mag. B*, 1987, **55**, 507.
16. Bernaerts, D., Zhang, X.B., Zhang, X.F., Amelinckx, S., Van Tendeloo, G., Van Landuyt, J., Ivanov, V. and Nagy, J.B., *Phil. Mag.*, 1995, **71**, 605.
17. Zhang, X.F. and Zhang, Z., *Phys. Rev. B*, 1995, **52**, 5313.
18. Chico, L., Crespi, V.H., Benediet, L.X., Louie, S.G. and Cohen, M.L., *Phys. Rev. Lett.*, 1996, **76**, 971.
19. Saito, R., Dresselhaus, G. and Dresselhaus, M.S., *Phys. Rev. B*, 1996, **53**, 2044.
20. Charlier, J.C., Ebbesen, T.W. and Lambin, Ph., *Phys. Rev. B*, 1996, **53**, 11108.
21. Lambin, Ph., Fonseca, A., Vigneron, J.P., Nagy, J.B. and Lucas, A.A., *Chem. Phys. Lett.*, 1995, **245**, 85.
22. Borštnik, B. and Lukman, D., *Fullerene Sci. Technol.*, 1994, **2**, 357.
23. Langer, L., Bayot, V., Grivei, E., Issi, J.P., Heremans, J.P., Olk, C.H., Stockman, L., Van Haesendonck, C. and Bruynseraede, Y., *Phys. Rev. Lett.*, 1996, **76**, 479.
24. Dai, H., Wong, E.W. and Lieber, C.M., *Science*, 1996, **272**, 523.
25. Blase, X., Charlier, J. C., De Vita, A., Car, R., *Appl. Phys. Lett.*, 1997, **70**, 197.
26. Hiura, H., Ebbesen, T.W., Fujita, J., Tanigaki, K. and Takada, T., *Nature*, 1994, **367**, 148.
27. Charlier, J.C., Lambin, Ph. and Ebbesen, T.W., *Phys. Rev. B*, 1996, **54**, R8377.
28. Ebbesen, T.W., *Phys. Today*, 1996, **49 (6 (June))**, 26.
29. Tersoff, J. and Ruoff, R.S., *Phys. Rev. Lett.*, 1994, **73**, 676.
30. Tominek, D. and Louie, S.G., *Phys. Rev. B*, 1988, **37**, 8327.
31. The $V_{pp\pi}$, interaction is here ~20% smaller than the experimental value of graphite used above, which reduces the band gap by the same proportion.
32. Blase, X., Benedict, L.X., Shirley, E.L. and Louie, S.G., *Phys. Rev. Lett.*, 1994, **72**, 1878.